A

Differentially expressed genes	ccRCCs	NKTs
Total	199	280
Up-regulated	125	46
Down-regulated	74	234

Pearson's Chi-squared test: P<2.2e-16

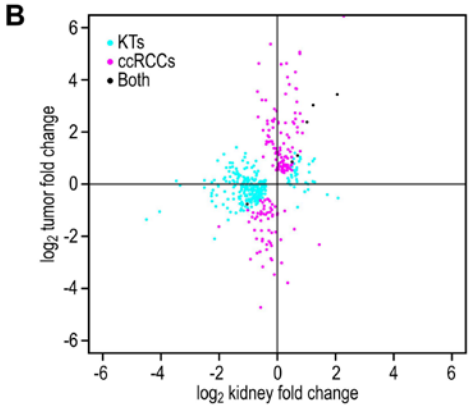

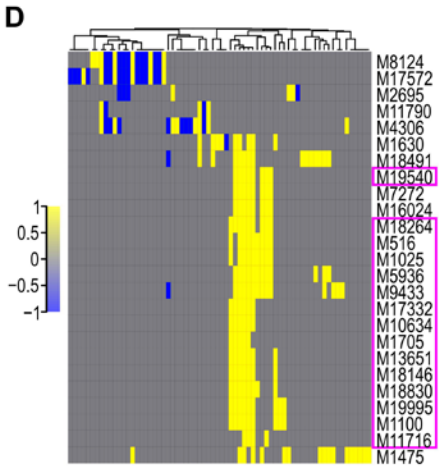

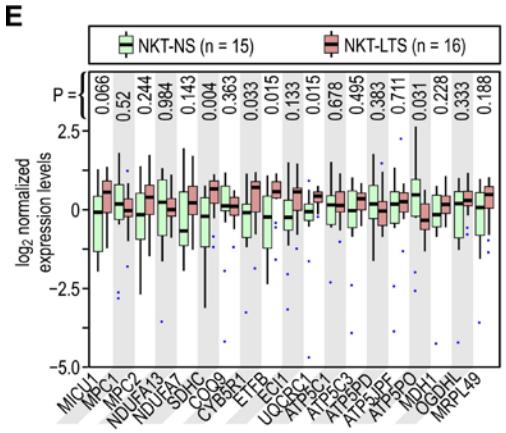

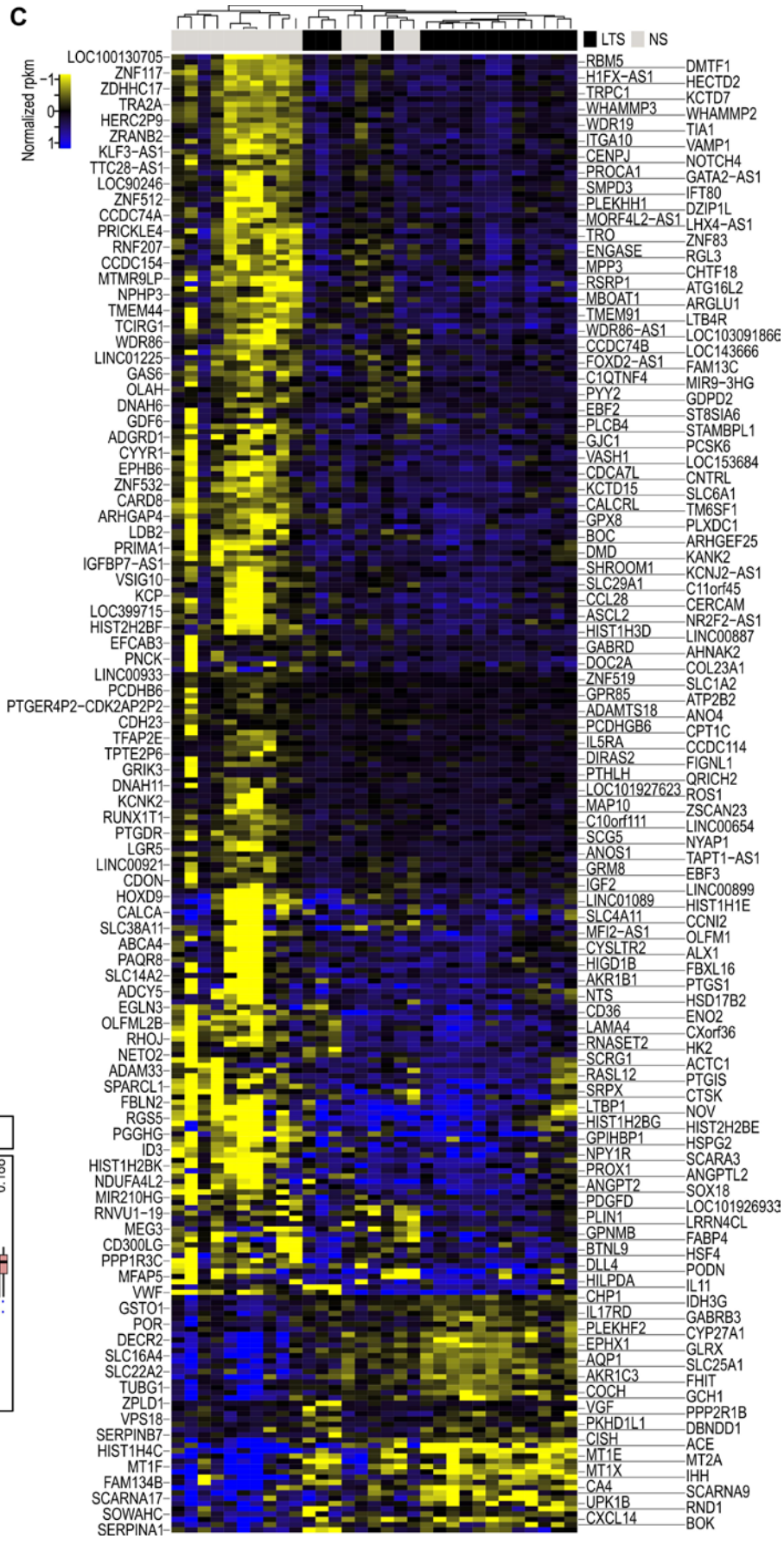

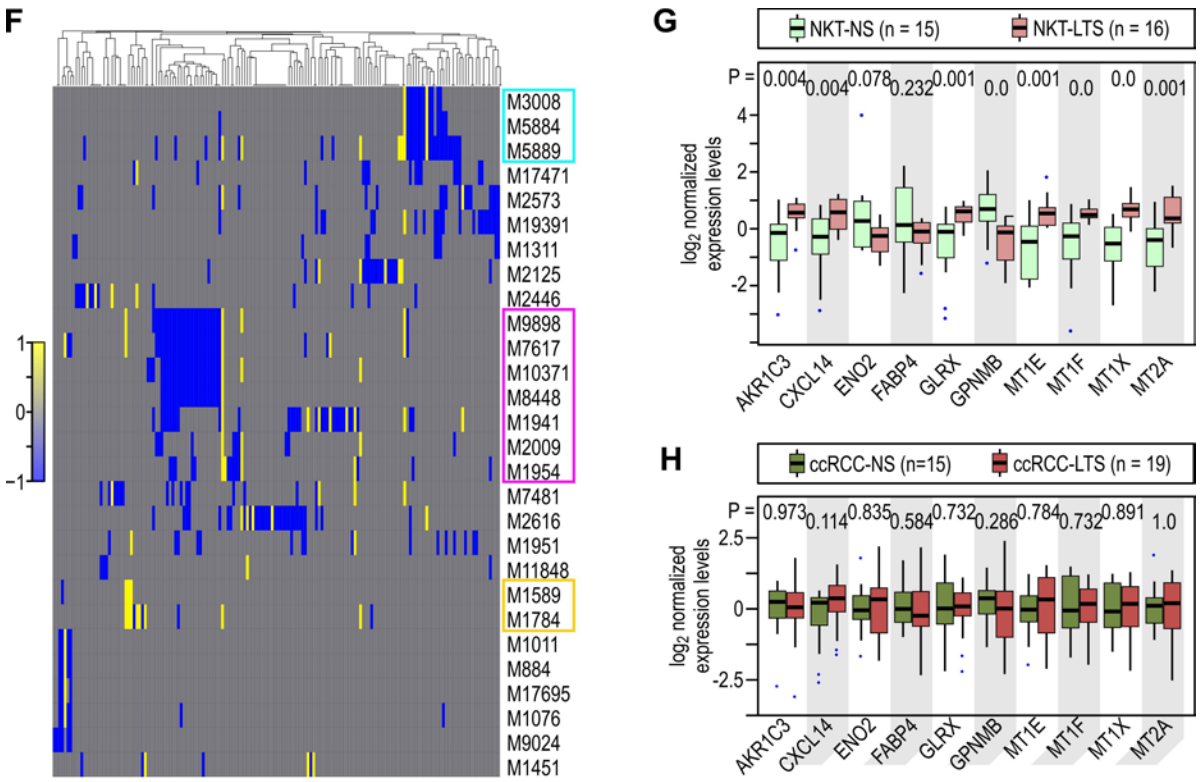

Supplemental Figure 1. Analysis of genes differentially regulated by TS in ccRCCs and NKTs. (**A**) Numbers of genes differentially regulated in ccRCC and NKTs from LTS compared to NS. (**B**) Lack of overlap between genes regulated differentially by TS in ccRCCs and NKTs. (**C**) Heatmap of all differentially regulated genes in NKTs from LTS compared to NS showing stratification with TS (marked by black in the top bar). Four samples from LTS stratified with NS. (**D**) Heatmap of pathways regulated by TS in ccRCCs. Magenta boxes on the right of the heatmap mark the GSEA mitochondrial/oxidative phosphorylation categories. See Supplemental Table 2C for definitions of the categories. (**E**) Box-whisker plots for expression of mitochondrial genes in NKTs from NS and LTS. The boxes represent lower and upper quartiles separated by the median (thick horizontal line) and the whiskers extend to the minimum and maximum values, excluding points that are outside the 1.5 interquartile range from the box (marked as circles). P values from Mann-Whitney-Wilcoxon test are provided at the top. (**F**) Heatmap of pathways regulated by TS in NKTs. Boxes on the right of the heatmap mark the GSEA categories including genes included in the response to arsenic (yellow), genes regulated by PRC2 (magenta), and extracellular matrix regulatory genes (blue). See Supplemental Table 3C for definition of GSEA categories. (**G**) Box-whisker plots and P values from Mann-Whitney-Wilcoxon test for expression of arsenic response genes in NKTs from NS and LTS. (**H**) Box-whisker plots and P values from Mann-Whitney-Wilcoxon test for expression of arsenic response genes in ccRCCs from NS and LTS. NKTs from 15 NS and 16 LTS were analyzed.

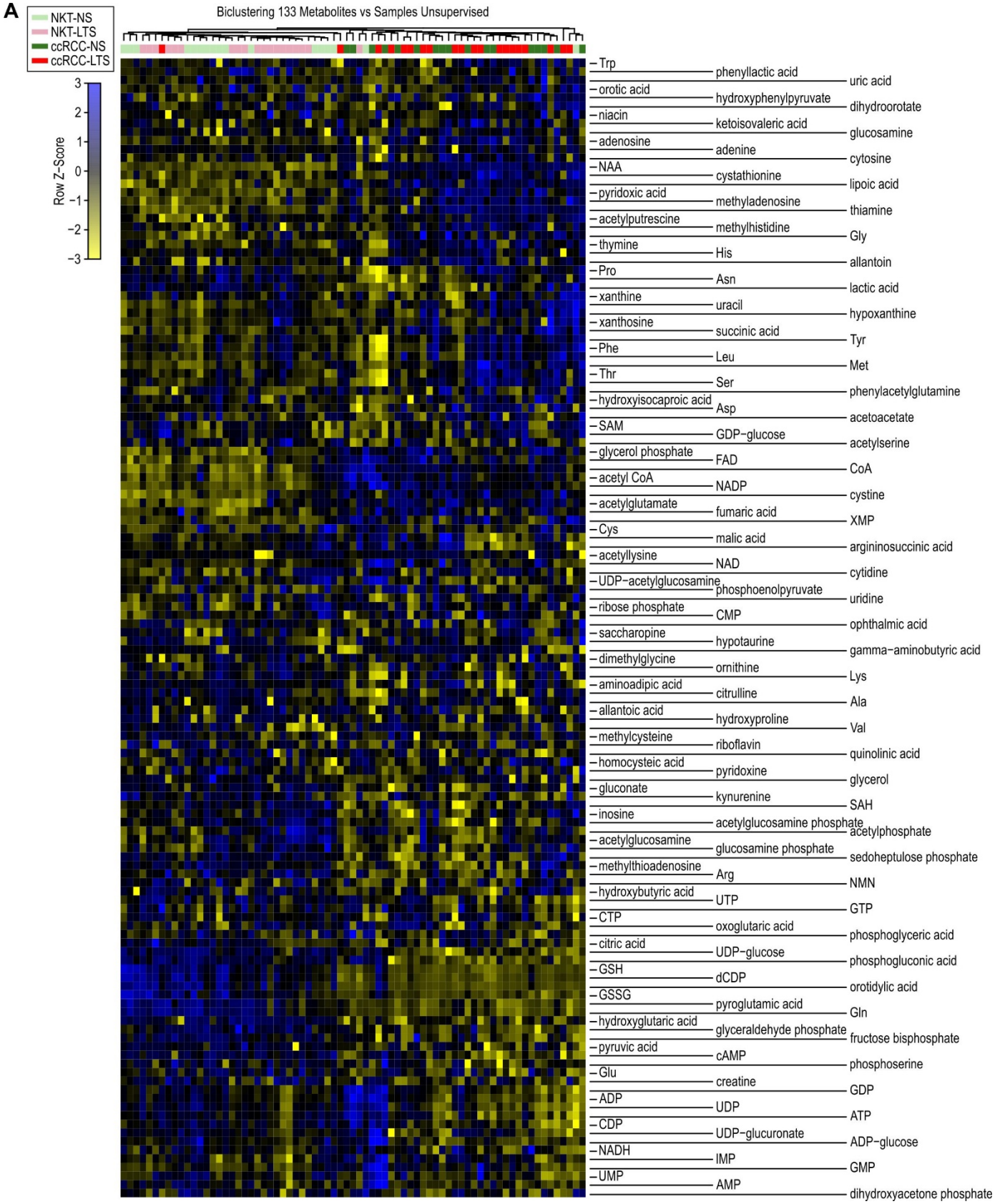
A
Biclustering 133 Metabolites vs Samples Unsupervised
NKT-NS
NKT-LTS
ccRCC-NS
ccRCC-LTS
Row Z-Score
3
2
1
0
−1
−2
−3
Trp
phenyllactic acid
uric acid
orotic acid
hydroxyphenylpyruvate
dihydroorotate
niacin
ketoisovaleric acid
glucosamine
adenosine
adenine
cytosine
NAA
cystathionine
lipoic acid
pyridoxic acid
methyladenosine
thiamine
acetylputrescine
methylhistidine
Gly
thymine
His
allantoin
Pro
Asn
lactic acid
xanthine
uracil
hypoxanthine
xanthosine
succinic acid
Tyr
Phe
Leu
Met
Thr
Ser
phenylacetylglutamine
hydroxyisocaproic acid
Asp
acetoacetate
SAM
GDP−glucose
acetylserine
glycerol phosphate
FAD
CoA
acetyl CoA
NADP
cystine
acetylglutamate
fumaric acid
XMP
Cys
malic acid
argininosuccinic acid
acetyllysine
NAD
cytidine
UDP−acetylglucosamine
phosphoenolpyruvate
uridine
ribose phosphate
CMP
ophthalmic acid
saccharopine
hypotaurine
gamma−aminobutyric acid
dimethylglycine
ornithine
Lys
aminoadipic acid
citrulline
Ala
allantoic acid
hydroxyproline
Val
methylcysteine
riboflavin
quinolinic acid
homocysteic acid
pyridoxine
glycerol
gluconate
kynurenine
SAH
inosine
acetylglucosamine phosphate
acetylphosphate
acetylglucosamine
glucosamine phosphate
sedoheptulose phosphate
methylthioadenosine
Arg
NMN
hydroxybutyric acid
UTP
GTP
CTP
oxoglutaric acid
phosphoglyceric acid
citric acid
UDP−glucose
phosphogluconic acid
GSH
dCDP
orotidylic acid
GSSG
pyroglutamic acid
Gln
hydroxyglutaric acid
glyceraldehyde phosphate
fructose bisphosphate
pyruvic acid
cAMP
phosphoserine
Glu
creatine
GDP
ADP
UDP
ATP
CDP
UDP−glucuronate
ADP−glucose
NADH
IMP
GMP
UMP
AMP
dihydroxyacetone phosphate

B

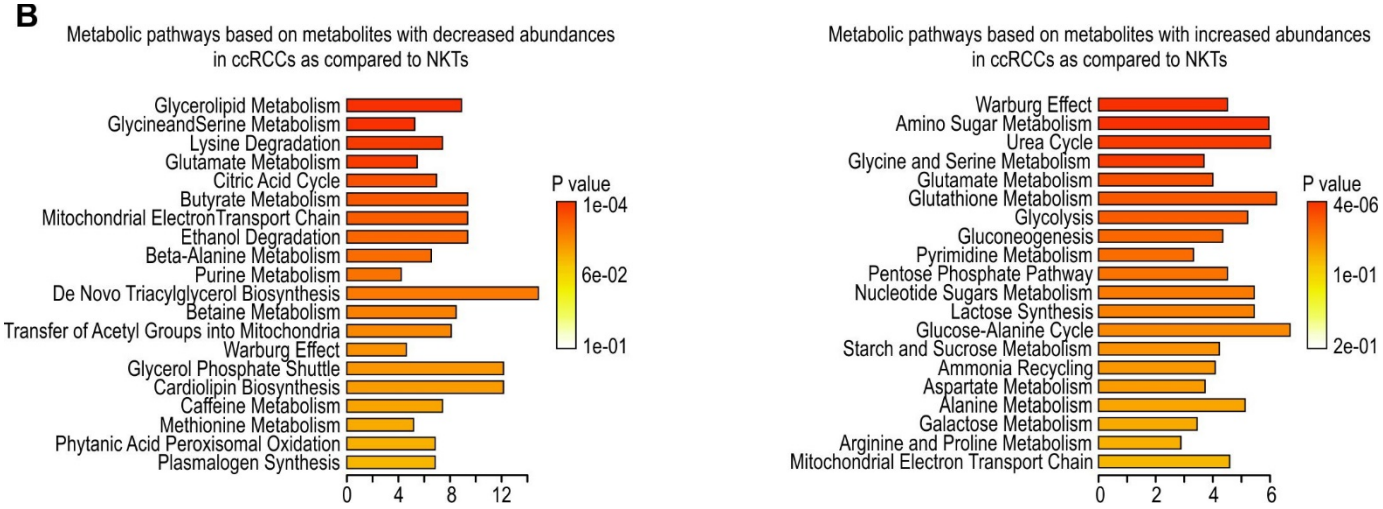

Supplemental Figure 2. Analysis of metabolites' steady-state levels in ccRCCs and NKTs from LTS and NS. (**A**) Heatmap of all differentially abundant metabolites showing stratification with tissue type but not with smoking status. (**B**) Metabolic pathways enriched for metabolites with differential abundance in ccRCCs and NKTs.

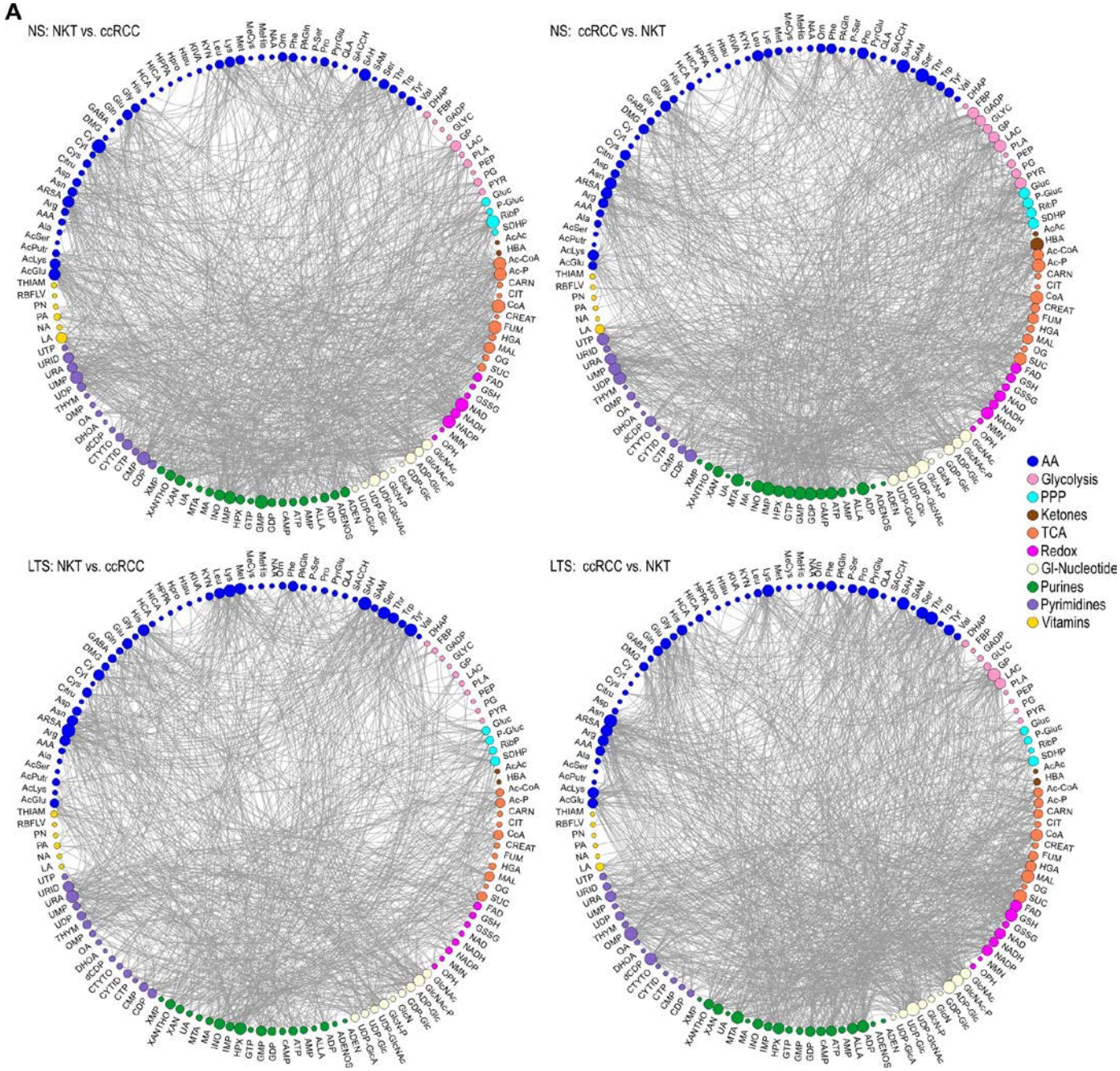
A
NS: NKT vs. ccRCC
NS: ccRCC vs. NKT
LTS: NKT vs. ccRCC
LTS: ccRCC vs. NKT
AA
Glycolysis
PPP
Ketones
TCA
Redox
Gl-Nucleotide
Purines
Pyrimidines
Vitamins

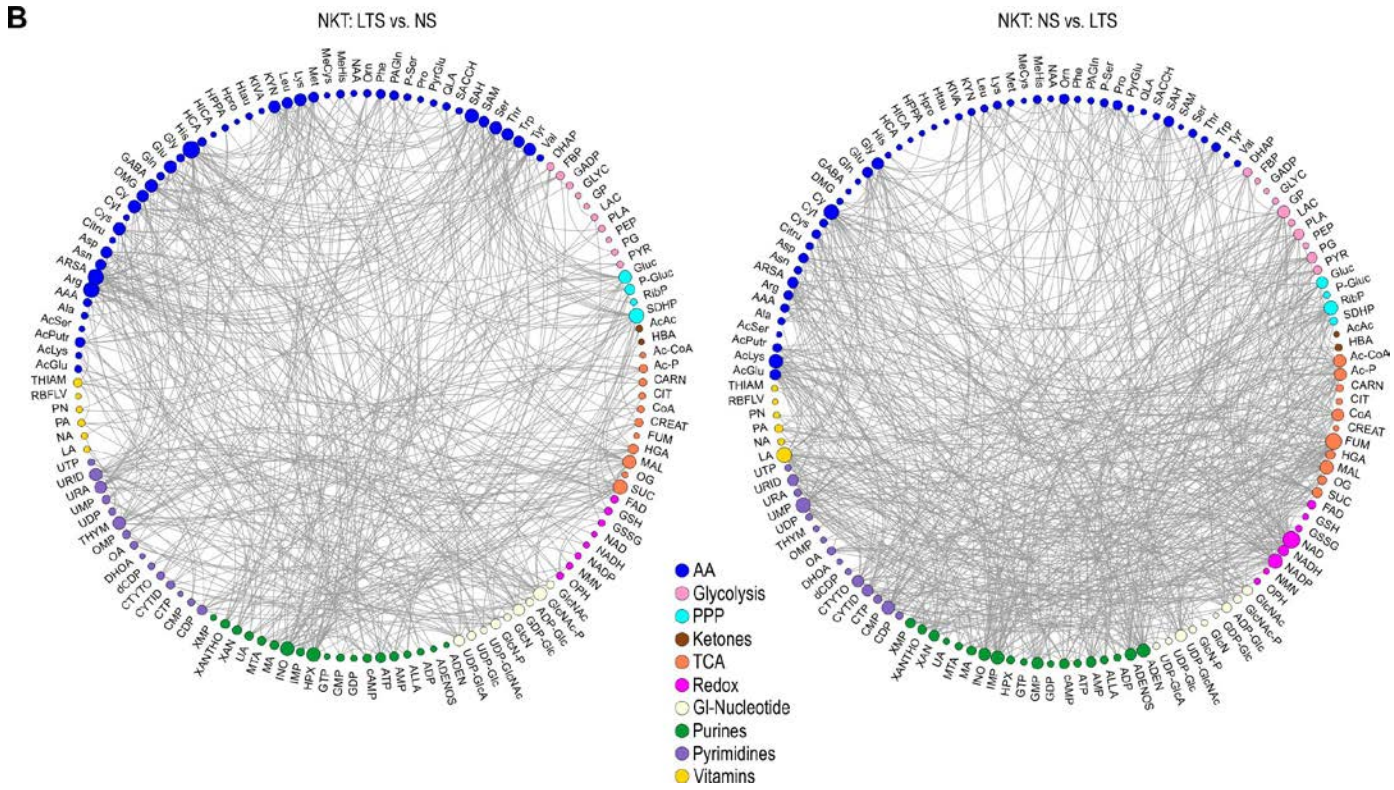

Supplemental Figure 3. Alterations in the intercorrelations of metabolites. (**A**) Circos showing unique edges for Spearman correlations among 133 metabolites with Spearman correlation coefficient ≥0.5 comparing NKTs and ccRCCs in NS and LTS. (**B**) Circos showing unique edges for Spearman correlations among 133 metabolites comparing NKTs from NS and LTS.

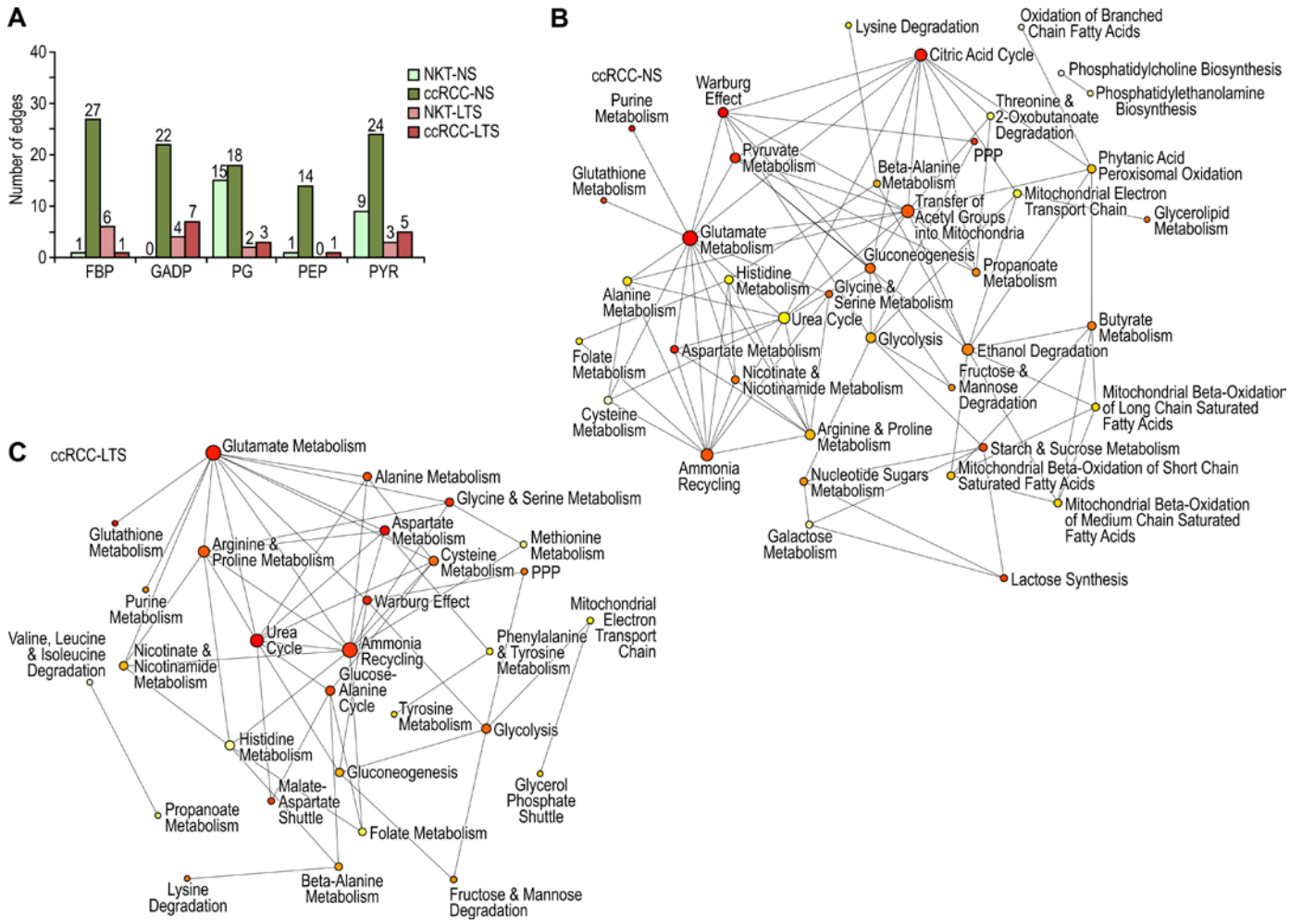

Supplemental Figure 4. Reprogramming of glycolytic metabolism in ccRCCs from LTS. (**A**) Bar graph showing the number of correlations for each individual glycolytic intermediate for each tissue shown in Fig. 4C, left. Numbers above the bars indicate number of correlations. (**B**) Enrichment analysis of pathways associated with metabolites correlated with glycolytic intermediates in ccRCCs from NS using MetaboAnalyst. (**C**) Enrichment analysis of pathways associated with metabolites correlated with glycolytic intermediates in ccRCCs from LTS using MetaboAnalyst.

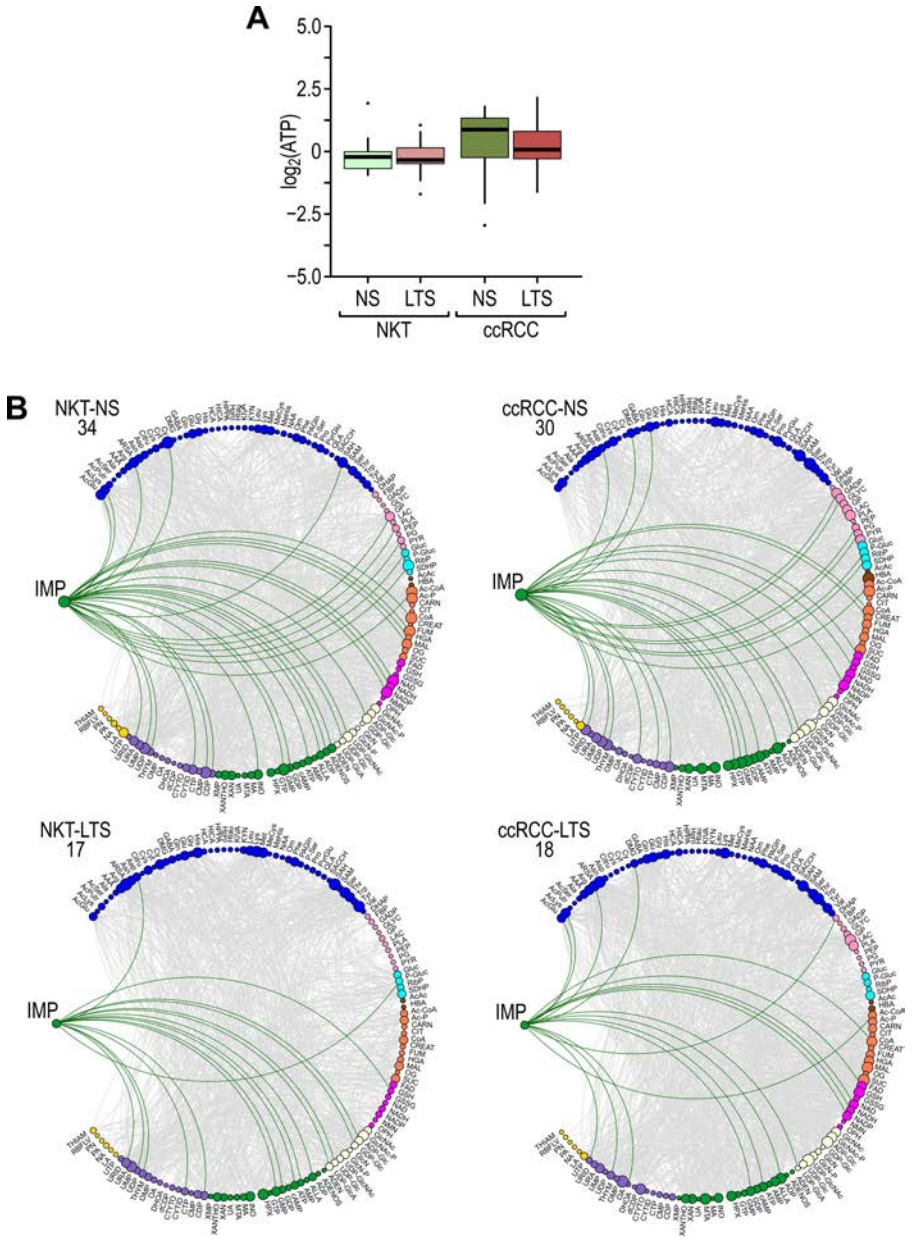

Supplemental Figure 5. Reprogramming of purine connections in ccRCCs from LTS. (**A**) Box-whisker plots of ATP concentration in NKTs and ccRCCs from NS and LTS. (**B**) Circos showing correlations of IMP in NKTs and tumors from NS and LTS. Numbers indicate number of correlations in each tissue.

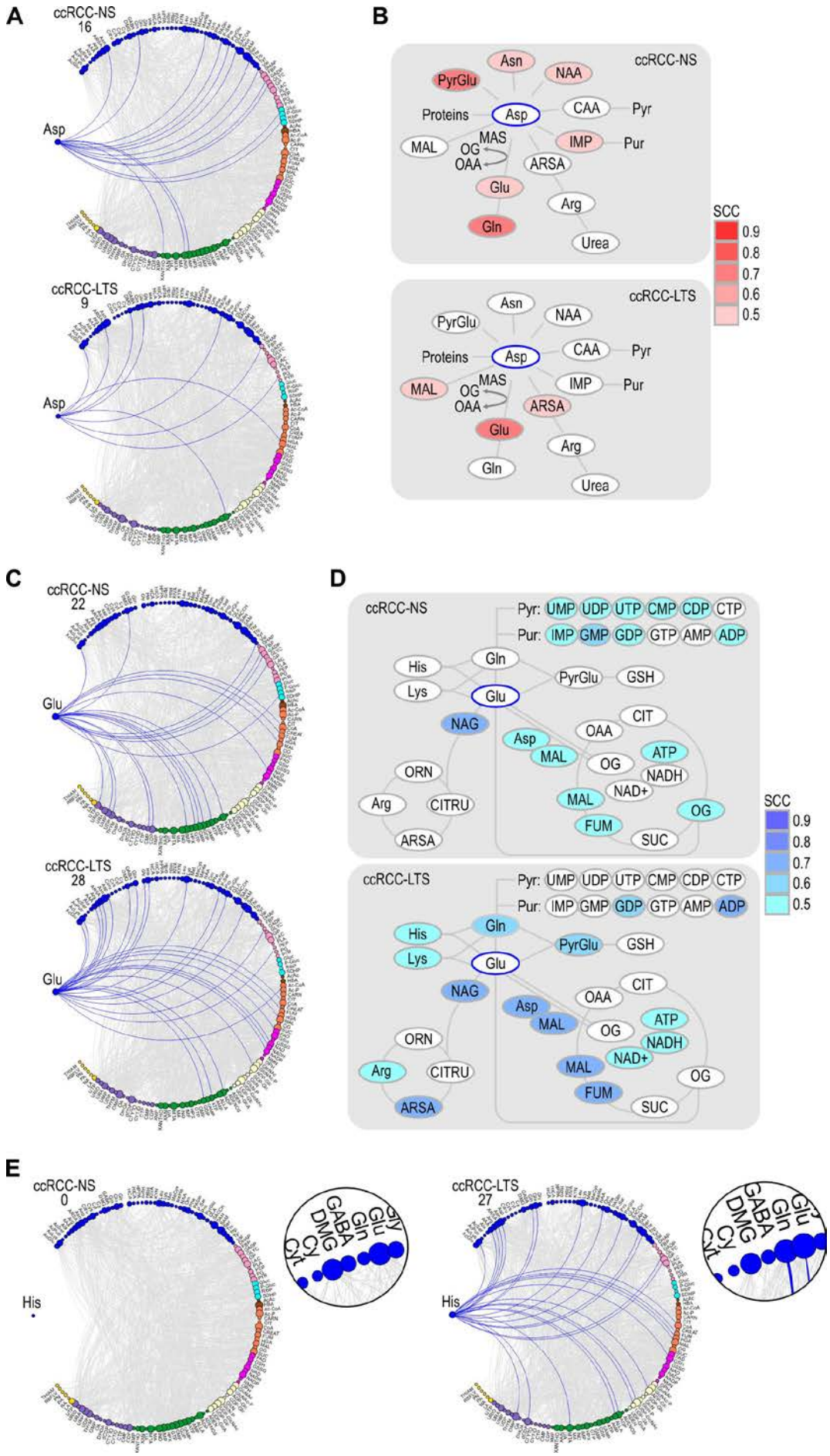
A
ccRCC-NS
16
Asp
ccRCC-LTS
9
Asp
B
ccRCC-NS
Asn
NAA
PyrGlu
Proteins
Asp
CAA
Pyr
MAL
MAS
OG
OAA
IMP
Pur
ARSA
Glu
Arg
Gln
Urea
ccRCC-LTS
Asn
NAA
PyrGlu
Proteins
Asp
CAA
Pyr
MAL
MAS
OG
OAA
IMP
Pur
ARSA
Glu
Arg
Gln
Urea
SCC
0.9
0.8
0.7
0.6
0.5
C
ccRCC-NS
22
Glu
ccRCC-LTS
28
Glu
D
ccRCC-NS
Pyr: UMP UDP UTP CMP CDP CTP
Pur: IMP GMP GDP GTP AMP ADP
His
Lys
Gln
Glu
PyrGlu
GSH
NAG
CIT
OAA
Asp
MAL
ATP
OG
NADH
ORN
NAD+
Arg
CITRU
MAL
OG
FUM
ARSA
SUC
ccRCC-LTS
Pyr: UMP UDP UTP CMP CDP CTP
Pur: IMP GMP GDP GTP AMP ADP
His
Lys
Gln
Glu
PyrGlu
GSH
NAG
CIT
OAA
Asp
MAL
ATP
OG
NADH
ORN
NAD+
Arg
CITRU
MAL
OG
FUM
ARSA
SUC
SCC
0.9
0.8
0.7
0.6
0.5
E
ccRCC-NS
0
His
Gly
Glu
Gln
GABA
DMG
Cy
Cyt
ccRCC-LTS
27
His
Glu
Gln
GABA
DMG
Cy
Cyt

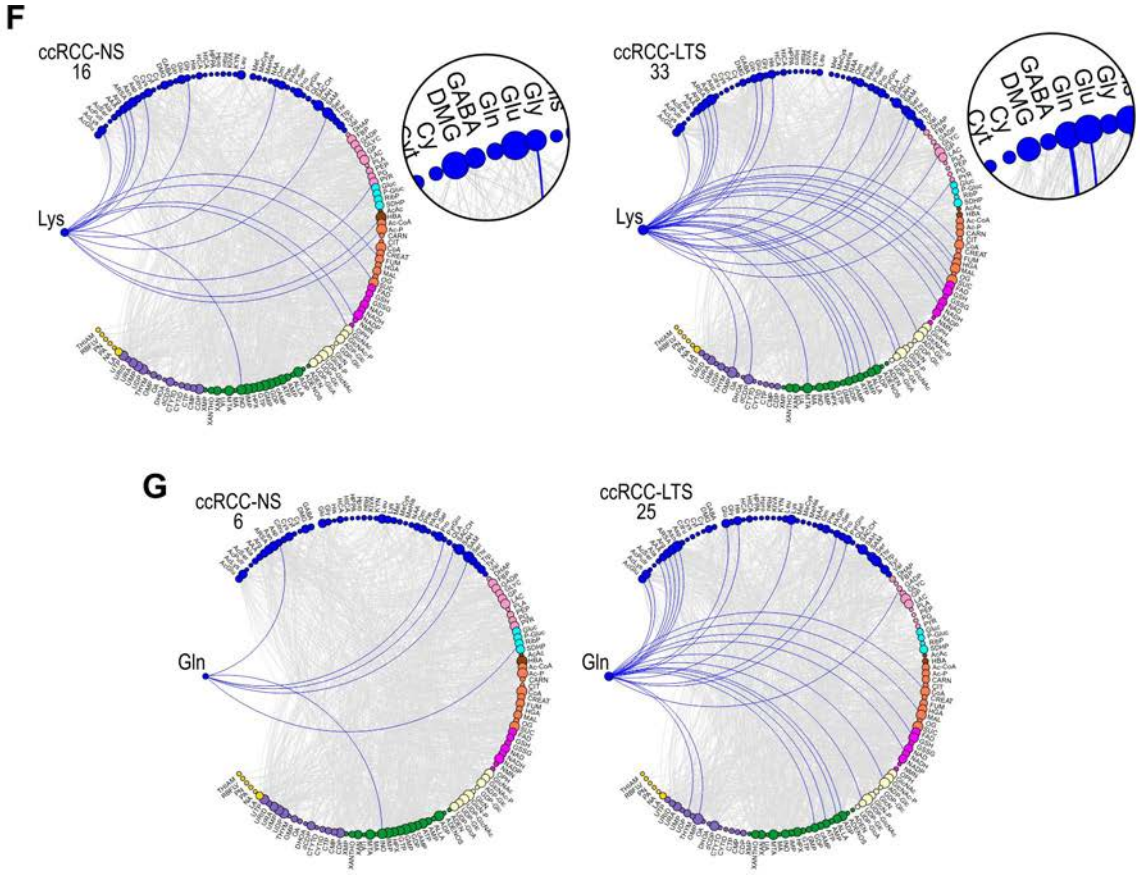
F
ccRCC-NS
16
Lys
Gly
Glu
Gln
GABA
DMG
Cy
Cyt
ccRCC-LTS
33
Lys
Gly
Glu
Gln
GABA
DMG
Cy
Cyt
G
ccRCC-NS
6
Gln
ccRCC-LTS
25
Gln

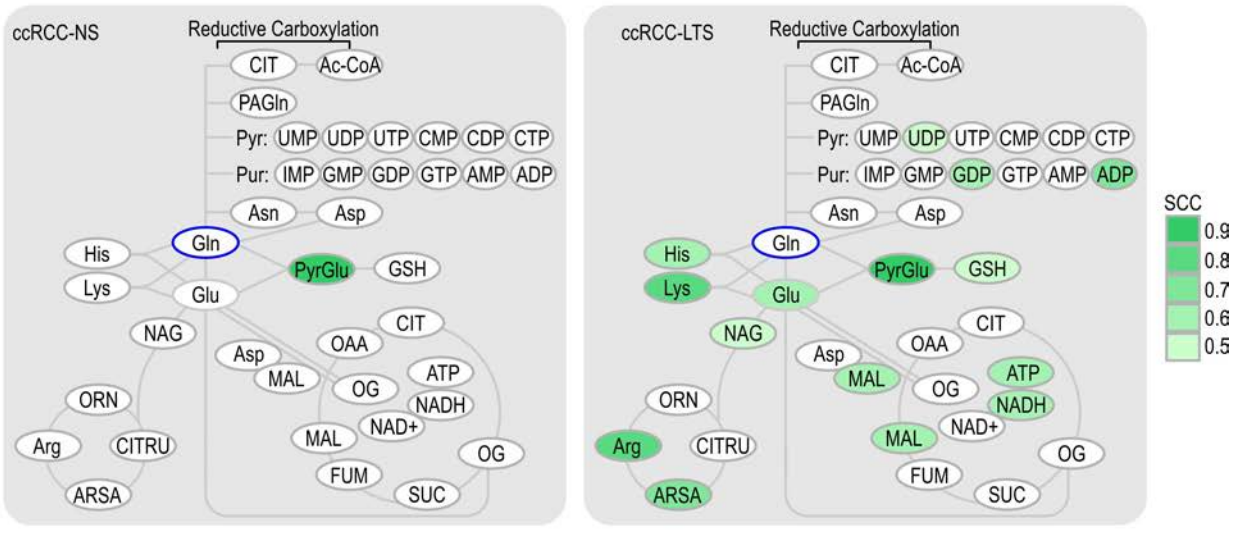
H
ccRCC-NS
Reductive Carboxylation
CIT
Ac-CoA
PAGln
Pyr: UMP UDP UTP CMP CDP CTP
Pur: IMP GMP GDP GTP AMP ADP
Asn
Asp
Gln
His
Lys
Glu
PyrGlu
GSH
NAG
CIT
OAA
Asp
MAL
ATP
OG
NADH
ORN
NAD+
Arg
CITRU
MAL
OG
FUM
ARSA
SUC
ccRCC-LTS
Reductive Carboxylation
CIT
Ac-CoA
PAGln
Pyr: UMP UDP UTP CMP CDP CTP
Pur: IMP GMP GDP GTP AMP ADP
Asn
Asp
Gln
His
Lys
Glu
PyrGlu
GSH
NAG
CIT
OAA
Asp
MAL
ATP
OG
NADH
ORN
NAD+
Arg
CITRU
MAL
OG
FUM
ARSA
SUC
SCC
0.9
0.8
0.7
0.6
0.5

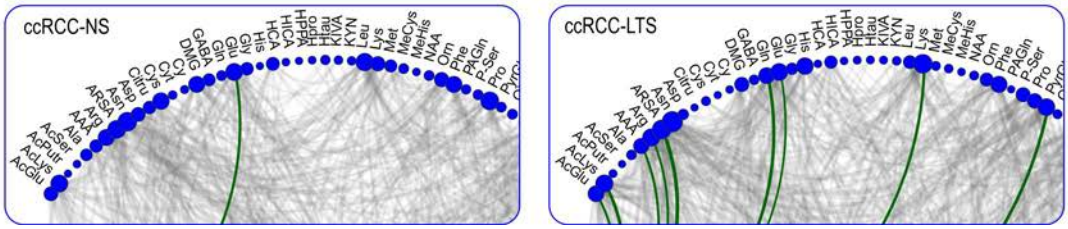
I
ccRCC-NS
ccRCC-LTS

Supplemental Figure 6. Reprogramming of amino acid metabolism. (**A**) Circos showing correlation for Asp (blue edges) in ccRCCs from NS and LTS. (**B**) Schematic representation of pathways utilizing Asp. Metabolites correlated with Asp marked in pink. Legend represents values of Spearman correlation coefficient (SCC) for Asp. (**C**) Circos show correlation for Glu (blue edges) in ccRCCs from NS and LTS. (**D**) Schematic representation of pathways utilizing Glu. Metabolites correlated with Glu marked in blue. Legend represents values of SCC for Glu. (**E**) Circos show correlations of His (blue edges) with other metabolites in ccRCCs from NS and LTS. (**F**) Circos show correlations of Lys (blue edges) with other metabolites in ccRCCs from NS and LTS. (**G**) Circos show correlations of Gln (blues edges) with other metabolites in ccRCCs from LTS and NS (**H**) Schematic representation of Gln metabolic connections in ccRCCs from NS and LTS. Green scale represents values of SCC for Gln. (**I**) Inserts derived from the Circos shown in Fig. 5A show correlations of ATP (green edges) with amino acid in ccRCC from NS and LTS. Numbers above all Circos indicate number of edges in the indicated tissues.

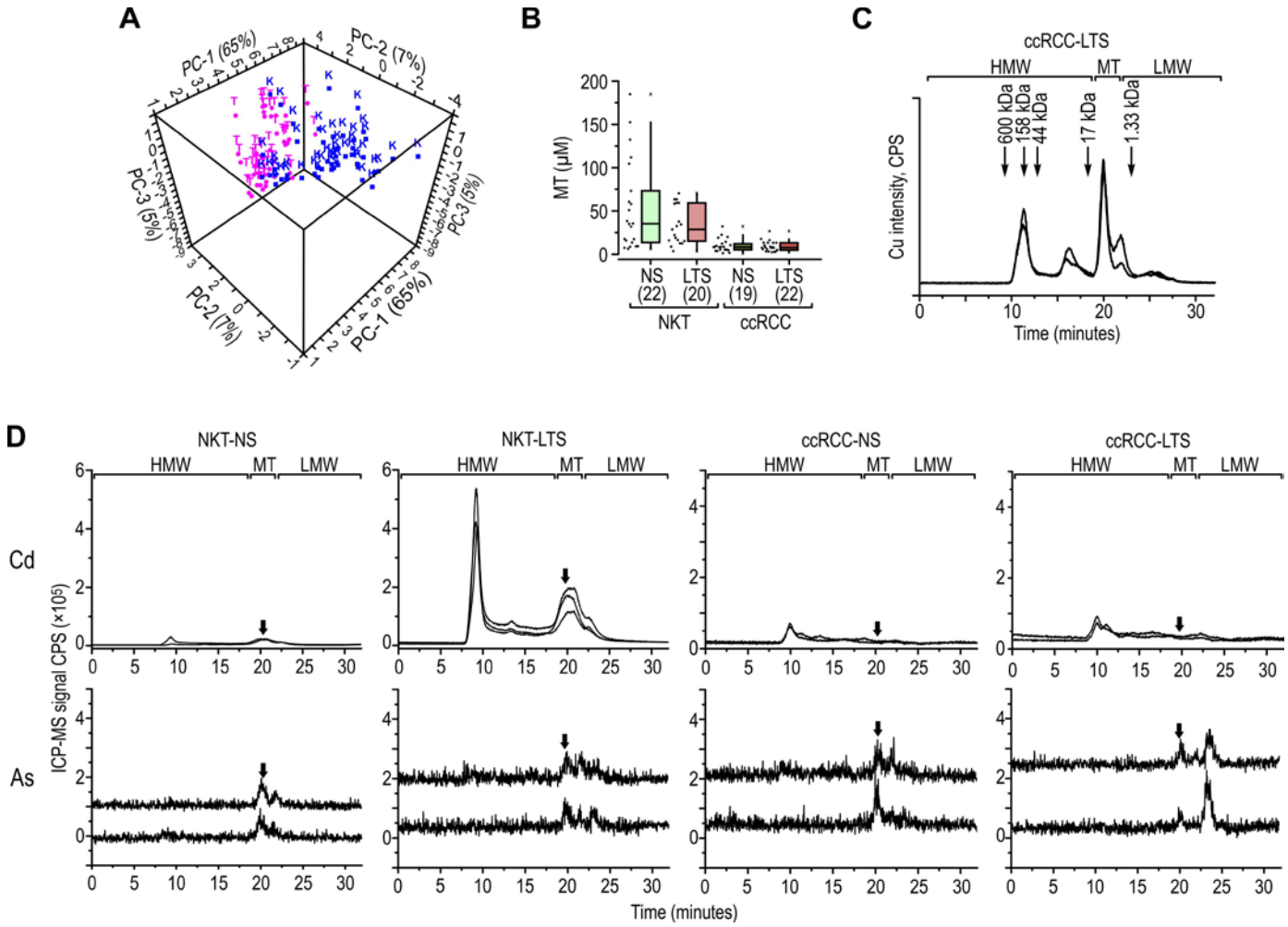

Supplemental Figure 7. Metallomic analysis of TS effects in NKTs and ccRCCs from NS and LTS. (**A**) Principal component analysis showing different distribution of metals between NKTs (blue) and ccRCCs (red). (**B**) Levels of MT in NKTs and ccRCCs from NS and LTS. (**C**) SEC-ICP-MS chromatogram shown in Fig. 6E. Arrows indicate retention times for the molecular weight standards used to calibrate the SEC column size. (**D**) SEC-ICP-MS chromatograms from indicated tissues for Cd and As. Y-axis on the left represents the intensity of signal for the metals. HMW- high molecular weight fraction, LMW- low molecular weight fraction, MT- metallothioneins.

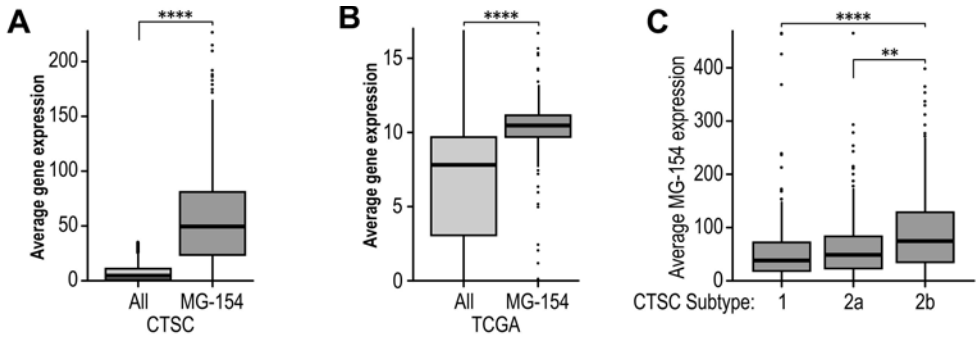

D

TCGA \ CTSC	1	2a	2b
1			
2	80%		
3		7.7%	100%
4			
5		30.8%	
6	20%	61.5%	

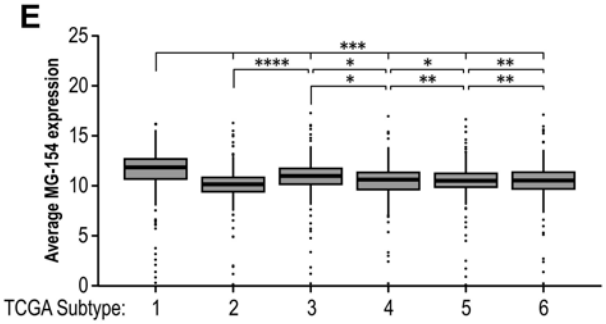

F

Comparisons	P-values
tcga_s1_vs_s2	5.67E-12
tcga_s1_vs_s3	7.91E-05
tcga_s1_vs_s4	2.89E-08
tcga_s1_vs_s5	1.14E-08
tcga_s1_vs_s6	4.19E-08
tcga_s2_vs_s3	8.12E-07
tcga_s2_vs_s4	0.012562
tcga_s2_vs_s5	0.013306
tcga_s2_vs_s6	0.008857
tcga_s3_vs_s4	0.014964
tcga_s3_vs_s5	0.004011
tcga_s3_vs_s6	0.009438
tcga_s4_vs_s5	0.765094
tcga_s4_vs_s6	0.949494
tcga_s5_vs_s6	0.794549

Supplemental Figure 8. Identification of ccRCC subtypes based on stratification using metabolic set of genes. (**A**) Box Whisker plots showing distribution of average expression of MG-154 (right) compared to the distribution of average expression of all genes (18,161) (left) measured in transcriptomics analysis in the entire TS cohort. $P=3.72e^{-71}$ (Wilcoxon test). (**B**) Box Whisker plots showing distribution of average expression of MG-154 (right) compared to the distribution of average expression of all genes (left) in the TCGA cohort of 309 Caucasian males. $P=3.51e^{-42}$ (Wilcoxon test). Note that TS and TCGA cohorts were processed and normalized differently resulting in different scales for expression values without affecting analysis of relative expression levels. (**C**) Box Whisker plots showing distribution of average expression of MG-154 in the three subtypes identified in the CTSC cohort. ****$P=1.98e^{-05}$, **$P=0.0052$ (Wilcoxon test). (**D**) Percent similarity between indicated CTSC and TCGA subtypes determined by the nearest centroid approach. (**E**) Box Whisker plots showing distribution of average expression of MG-154 in the six subtypes identified in TCGA cohort. (**F**) P values determined by Wilcoxon test for all the comparison among 6 TCGA subtypes.

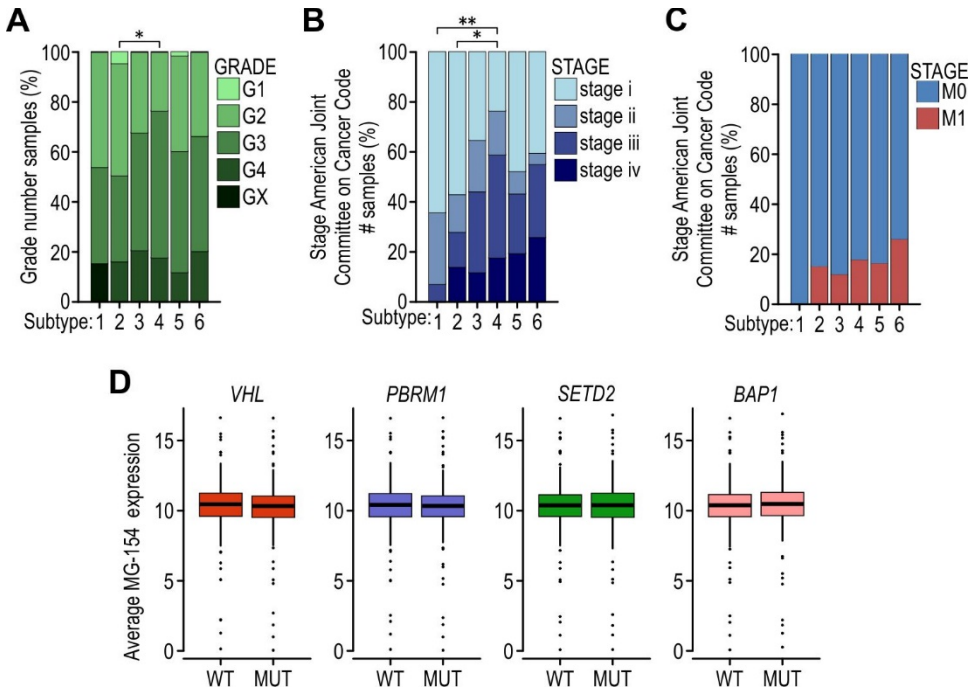

Supplemental Figure 9. Characterization of metabolic subtypes in TCGA. (**A**) Stacked bar graphs showing distribution of tumor grades among 6 TCGA subtypes. The only significant difference in G2+G1 vs. G3+G4 is between subtypes 4 and 2. *, P=0.02 (chi-square). (**B**) Stacked bar graphs showing distribution of tumor stage among 6 subtypes. There is a significant difference in stage I+II vs III+IV in subtype 4 when compared to subtype 2 and 1. *, P=0.028, ***, P=0.008 (chi-square test). (**C**) Stacked bar graph showing status of metastases in the indicated subtype. M0- no distant metastases; M1- metastatic spread to different tissues. There is no difference between subtype 4 and other subtypes. (**D**) Average expression of MG-154 in TCGA tumors with either wild type or mutated indicted tumor suppressor genes.